Approximations Method for Space Frame Synthesis

W. C. Mills-Curran,* R. V. Lust,† and L. A. Schmit‡
The University of California, Los Angeles, California

A method is presented for the minimum mass design of three-dimensional space frames constructed of thin-walled rectangular cross-sectional members. Constraints on nodal displacements and rotations, material stress, local buckling, and cross-sectional dimensions are included. A high-quality separable approximate problem is formed in terms of the reciprocals of the four section properties of the frame element cross section, replacing all implicit functions with simplified explicit relations. The cross-sectional dimensions are efficiently calculated without using multilevel techniques. Several test problems are solved, demonstrating that a series of approximate problem solutions converge rapidly to an optimal design.

I. Introduction

THIS paper reports on a new approach and capability for the optimization of three-dimensional space frame type structures with nonstandardized element cross sections. The mass of the structure is to be minimized subject to constraints which include nodal displacements and rotations, material stress, local buckling, and design variable side constraints. The structure is represented by a finite element model using a twelve degree of freedom (two end nodes, with three displacements and three rotations per node) frame element. Figure 1 details the rectangular, thin-walled, doubly symmetric cross section for the ith element.

A separable approximate problem is formed using reciprocal section properties (RSP's)—the inverse of an element's cross-sectional area and polar and bending moments of inertia (i.e., $X_{i1}=1/A_i$; $X_{i2}=1/J_i$; $X_{i3}=1/I_{zzi}$; $X_{i4}=1/I_{yyi}$). These approximations are of high quality when formed in terms of the RSP's, due to the algebraic form of the actual problem statement. Side constraints on the cross-sectional dimensions (CSD's) are reflected into RSP space by means of an approximate relationship between these two sets of variables. The form of this approximate relationship is tailored to take advantage of the strengths of the selected optimizer.

One of two optimizers may be selected to solve the approximate problem. The first is NEWSUMT, an extended quadratic interior penalty function optimizer.[1] The second is DUAL2, a dual space optimizer that maximizes the dual function by a second-order method.[2]

These problem solving capabilities are combined in a self-contained Fortran code which allows the user to optimize a general three-dimensional space frame structure modeled with frame elements of thin-walled rectangular cross section. Several example problems are solved, showing that this new approach to the frame problem is useful and efficient.

II. Background

In the past, frame optimization efforts have typically followed one of two paths. The first and most common method is oriented toward civil engineering applications, and is identified by the use of an approximate relationship between section properties, for example,

$$I=cA^p \tag{1}$$

where c and p are constants, I the cross-sectional moment of inertia, and A the cross-sectional area.[3-6] The relationship represents an assumption governing the geometry of the cross section during redesign. Assumptions of this type are especially convenient when components are selected from standard sections and Eq. (1) is the result of a curve fit. This method has the advantage of representing the design of a structural element with only one design variable, resulting in efficient optimization techniques. However, in applications where structural elements are usually custom fabrications, as in the aerospace and auto industries, Eq. (1) restricts the freedom of design of the cross section, resulting in a mass penalty at the final design.

The restrictions of Eq. (1) can be overcome by selecting the cross-sectional dimensions as the design variables.[7,8] By posing the design problem in terms of the CSD's (or their inverse), the least mass design for a particular class of cross sections can be realized. Unfortunately, in the case of frame elements, the CSD's are not the variables of choice for forming approximations of behavior constraints, such as nodal displacements or material stresses. Behavior constraint approximations in terms of the CSD's are accurate over a relatively small range, requiring frequent reanalysis of the structure, and resulting in slowed convergence. Problems solved by this method usually require a relatively large number of iterations, and may also exhibit convergence difficulties.

III. Problem Statement

Objective Function

The objective function to be minimized is the mass of the structure;

$$\min_A M(A)=\min_A \sum_{b=1}^{\bar{B}} \rho_b L_b A_b \tag{2}$$

where M, ρ, L, and A are the structural mass, element material density, length, and cross-sectional area for the bth analysis element.

Behavior Constraints

Nodal displacements and rotations are determined by solving the equilibrium equations

$$[K]u=F \tag{3}$$

Presented as Paper 82-0682 at the AIAA/ASME/ASCE/AHS 23rd Structures, Structural Dynamics and Materials Conference, New Orleans, La., May 10-12, 1982; submitted May 12, 1982; revision received Jan. 19, 1983.

*Graduate Research Assistant; currently Member of Technical Staff, Sandia National Laboratories. Student Member AIAA.

†Graduate Research Assistant.

‡Professor of Engineering and Applied Science. Associate Fellow AIAA.

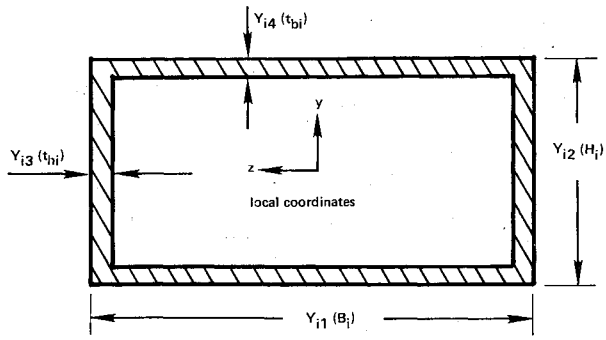

Fig. 1 Cross section of the *i*th element.

Upper and lower bounds on the *l*th nodal quantity are written

$$1-u_l/u_l^{(U)} \geq 0 \tag{4}$$

$$1-u_l/u_l^{(L)} \geq 0 \tag{5}$$

Note that Eq. (5) is written for a strictly negative lower bound.

Material stress constraints are evaluated by the von Mises stress criterion for plane stress

$$1-(1/\sigma_y^2)(\sigma^2+3\tau^2) \geq 0 \tag{6}$$

This stress constraint is evaluated at eight locations at each end node, so that 16 stress constraints are evaluated for each analysis element. The Appendix contains the detailed development of this constraint.

The local buckling constraint is constructed by modeling each box side as an infinitely long, simply supported plate, subjected to a linearly varying normal stress, and a shear stress as shown in Fig. 2. The buckling constraint is developed from the buckling interaction formula for the three stresses shown in Fig. 2[9]

$$1-R_x-R_b^2-R_s^2 \geq 0 \tag{7}$$

R_x, R_b, and R_s are the ratios of the applied stress to the critical buckling stress when no other stresses are present. Thus,

$$R_x=\sigma_x/\sigma_{xcr} \tag{8}$$

$$R_b=\sigma_b/\sigma_{bcr} \tag{9}$$

$$R_s=\tau/\tau_{cr} \tag{10}$$

Buckling constraints are written for each side of the box section at both end nodes, so that eight constraints are included for each analysis element. These buckling constraints are conservative because they neglect any stiffening effects of neighboring sides of the cross section and of neighboring structural elements. Further development of Eqs. (7-10) may be found in the Appendix.

Side Constraints

Upper- and lower-bound side constraints are written to prevent the CSD's from assuming undesirable proportions

$$1-Y_{ik}/Y_{ik}^{(U)} \geq 0; \qquad i=1,\ldots,B \quad k=1,2,3,4 \tag{11}$$

and

$$Y_{ik}/Y_{ik}^{(L)}-1 \geq 0; \qquad i=1,\ldots,B \quad k=1,2,3,4 \tag{12}$$

Because the cross-sectional design of several finite element analysis elements may be linked to form one design element, the number of design elements may be less than the number of analysis elements. Equations (11) and (12) represent eight constraints per design element for B design elements.

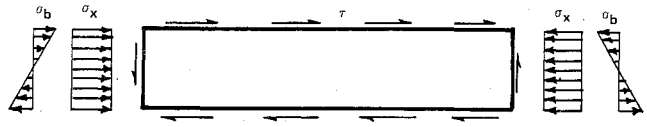

Fig. 2 Buckling stresses on a long simply supported plate.

Implicit Problem Statement

In terms of the CSD variables, the mass of the structure is the objective function to be minimized, and may be symbolically expressed

$$\min_Y \bar{M}(Y) \tag{13}$$

where Y is the vector CSD variables Y_{ik}. Similarly, the behavior constraints of Eqs. (4-7), which include nodal displacements and rotations, material stress, and local skin buckling, are written for Q constraints

$$g_q(Y) \geq 0; \quad q=1,\ldots,Q \tag{14}$$

The P side constraints, Eqs. (11) and (12), on the CSD variables are also written

$$h_p(Y) \geq 0; \quad p=1,\ldots,P \tag{15}$$

It is important to note that the behavior constraints of Eqs. (14) require solution of the equilibrium equations, Eq. (3), for the nodal deflections and the element forces of the structure. As a result, Eqs. (14) are implicit functions of the CSD variables. Before proceeding with optimization of the structure, all implicit functions must be replaced by an explicit approximation.

IV. Approximate Problem Generation

In order to make the implicit problem stated in Eqs. (13-15) computationally tractable it is necessary to construct a series of explicit approximate problems. These approximate problems must be algebraically explicit and they should capture the essential features of the original implicit problem. Various approximate representations can be generated. For example, by employing reciprocal section properties as intermediate variables it is possible to construct high-quality explicit approximations for nodal displacement and rotation constraints. This is accomplished by introducing first-order Taylor series expansions for the nodal displacements in terms of the RSP's and then substituting closed-form expressions for the RSP's in terms of the cross-sectional dimensions. This approach leads to high-quality explicit approximations for the constraints on nodal displacements and rotations. Indeed, these expressions are exact for statically determinate frameworks. However, it is important to note that these approximations are highly nonlinear and nonseparable functions of the CSD's. On the other hand, using the CSD's as the optimizer variables leads to high-quality approximations for the local stress constraints and exact representation of the CSD side constraints. The alternative approach adopted in this paper selects the RSP's as the optimizer variables. The nodal displacement and rotation constraints are represented by linear approximations in terms of the RSP's. The local stress constraints and the CSD side constraints are then expressed approximately in terms of the RSP's. In this approach the advantage of having linear and separable approximations for the constraints is traded off against the reduced quality of the approximate representations for the local stress and CSD side constraints. The main

attractive feature of the approximate formulation in RSP space adopted here is that it leads to an optimization problem with a special algebraic form which can be treated using an efficient dual method optimizer. The following section elaborates on the approximations made in forming each appropriate problem for the optimizer.

Constraint Deletion

Equations (14) and (15) represent a large number of constraints, most of which are not potentially active. The efficiency of the optimizer and the approximate problem generator is improved if only critical and potentially active constraints are considered. The method used here is taken from the ACCESS-3 code.[10]

With user supplied values for the truncation reduction factor (TRF) and C, the truncation boundary value (TBV) is defined for the behavior constraints, Eqs. (14),

$$\text{TBV} = [\min_q \{g_q\} - C] \times \text{TRF} + C \tag{16}$$

All constraints which satisfy

$$g_q \le \text{TBV}; \quad q = 1,\ldots,Q \tag{17}$$

are retained for generation of approximate expressions which are passed to the optimizer.

Additionally, TRF is modified at each stage by the following relationship:

$$\text{TRF} = \min\{\text{TRF}_{\max}, \text{TRF} \times \text{TRF}_{\text{mult}}\} \tag{18}$$

where TRF_{mult} and $\text{TRF}_{\max}$ are user supplied. The side constraints of Eqs. (15) are similarly treated.

Nodal Response Approximation

The selection of appropriate intermediate variables can improve significantly the quality of a linear approximation. For membrane and truss element structures, it has been shown that the inverse of the element's thickness or area is the appropriate intermediate variable and can be expected to generate high-quality linear approximations of the nodal responses.[11] For example, in a membrane structure where t_i is the ith element thickness, the approximate relationship for the nodal displacement vector

$$u = u_0 + \sum_{i=1}^{I} \left.\frac{\partial u}{\partial\left(\frac{1}{t_i}\right)}\right|_{t=t_0} \left(\frac{1}{t_i} - \frac{1}{t_{0i}}\right) \tag{19}$$

is expected to be of high quality. Fuchs has shown that this favorable behavior follows from the fact that the nodal displacements are homogeneous functions of degree one in $1/t_i$, resulting in a linearization which is identical for all expansion points on a scaling line.[12] One then expects Eq. (19) to be exact along that scaling line.

For a twelve degree of freedom frame element, nodal displacements and rotations are homogeneous functions of degree one in the four reciprocal section properties. For the cross section shown in Fig. 1, the RSP's are defined as follows:

$$X_{i1} = \frac{1}{A_i} = \frac{1}{Y_{i1}Y_{i2} - (Y_{i2} - 2Y_{i4})(Y_{i1} - 2Y_{i3})} \tag{20}$$

$$X_{i2} = \frac{1}{J_i} = \frac{Y_{i2}Y_{i4} + Y_{i1}Y_{i3}}{2Y_{i1}^2 Y_{i2}^2 Y_{i3} Y_{i4}} \tag{21}$$

$$X_{i3} = \frac{1}{I_{zzi}} = \frac{12}{Y_{i1}Y_{i2}^3 - (Y_{i1} - 2Y_{i3})(Y_{i2} - 2Y_{i4})^3} \tag{22}$$

$$X_{i4} = \frac{1}{I_{yyi}} = \frac{12}{Y_{i2}Y_{i1}^3 - (Y_{i2} - 2Y_{i4})(Y_{i1} - 2Y_{i3})^3} \tag{23}$$

or symbolically

$$X_{ij} = f_{ij}(Y) \tag{24}$$

where X_{ij}, A_i, J_i, I_{zzi}, and I_{yyi} are, respectively, the jth RSP, the cross-sectional area, the polar moment of inertia, and the moments of inertia about the z and y axes, all for the ith design element. For the 12 degree of freedom frame element, the approximation corresponding to Eq. (19) is

$$u = u_0 + \sum_{i=1}^{B}\sum_{j=1}^{4} \left.\frac{\partial u}{\partial X_{ij}}\right|_{X=X_0} (X_{ij} - X_{0ij}) \tag{25}$$

Equation (25) is used to convert Eqs. (4) and (5) to explicit form, noting that any clearly inactive constraints are not considered. Equations (4) and (5) can then be expressed as a linear series of the form

$$\sum_{i=1}^{B}\sum_{j=1}^{4} C_{ijq}(X_{ij} - X_{0ij}) + C_{0q} \ge 0; \quad q = 1,\ldots,Q \tag{26}$$

Side Constraints

Using Eqs. (20-24) the side constraints of Eqs. (11) and (12) are brought into RSP space. Because the two optimizers (NEWSUMT and DUAL2) use significantly different techniques, the side constraint approximations are tailored for the specific optimizer selected by the designer.

NEWSUMT Form

Inspection of Eqs. (20-23) indicates that a linearization in terms of $1/X_{ij}$ is of higher quality than a linearization in terms of X_{ij}. An element of the Jacobian, thus, is defined from Eq. (24)

$$J_{ijk} = \frac{\partial[1/f_{ij}(Y_0)]}{\partial Y_{ik}} \tag{27}$$

Equation (24) is then approximated

$$\frac{1}{X_{ij}} = \frac{1}{X_{0ij}} + \sum_{k=1}^{4} J_{ijk}(Y_{ik} - Y_{0ik}) \tag{28}$$

Defining an element of the inverse of the ith Jacobian matrix as H_{ijk}, Eq. (28) is inverted

$$Y_{ik} = Y_{0ik} + \sum_{j=1}^{4} H_{ikj}\left(\frac{1}{X_{ij}} - \frac{1}{X_{0ij}}\right) \tag{29}$$

Equation (29) is substituted in Eqs. (11) and (12) to generate constraints of the form

$$\sum_{i=1}^{B}\sum_{j=1}^{4} B_{ijp}\left(\frac{1}{X_{ij}} - \frac{1}{X_{0ij}}\right) + B_{0p} \ge 0 \tag{30}$$

DUAL2 Form

To insure a convex problem statement, which is required for use of the dual method, the side constraints are formed with a linear approximation in terms of the RSP's. As in Eq. (27), define

$$\bar{J}_{ijk} = \frac{\partial[f_{ij}(Y_0)]}{Y_{ik}} \tag{31}$$

Equation (24) is then approximated

$$X_{ij} = X_{0ij} + \sum_{k=1}^{4} \bar{J}_{ijk}(Y_{ik} - Y_{0ik}) \tag{32}$$

Defining an element of the inverse of the ith Jacobian matrix as $\bar{H}_{ijk}$, Eq. (32) is inverted

$$Y_{ik} = Y_{0ik} + \sum_{j=1}^{4} \bar{H}_{ikj}(X_{ij} - X_{0ij}) \tag{33}$$

Equation (33) is substituted in Eqs. (11) and (12) to generate constraints of the form

$$\sum_{i=1}^{B}\sum_{j=1}^{4} \bar{B}_{ijp}(X_{ij} - X_{0ij}) + \bar{B}_{0p} \geq 0 \tag{34}$$

Stress and Buckling Constraints

The material stress and local buckling constraints are functions of both the RSP's and the CSD's of one design element, and of the nodal forces, which may be functions of the design variables of all other elements in the structure. In order to simplify the form of the approximate problem, and to limit the number of degrees of freedom for which Eq. (25) must be generated, the approximation of force invariance is made (i.e., the nodal forces do not vary as the structural design is changed). The forces are updated, however, after the solution of each approximate problem.

Representing the stress and buckling constraints of Eqs. (6) and (7) as $\tilde{g}_q(X,Y)$, a linear approximation is formed analytically

$$\hat{g}_q = \tilde{g}_q(X_0, Y_0) + \sum_{i=1}^{B}\sum_{j=1}^{4}\left[\frac{\partial \tilde{g}_q}{\partial X_{ij}} + \sum_{k=1}^{4}\frac{\partial \tilde{g}_q}{\partial Y_{ik}}\frac{\partial Y_{ik}}{\partial X_{ij}}\right]\Bigg|_{X_0,Y_0} \times (X_{ij} - X_{0ij}) \geq 0 \tag{35}$$

where the $\partial Y_{ik}/\partial X_{ij}$ are evaluated from Eq. (29) or (33) depending on which optimizer is selected. The resulting form of Eq. (35) is the same as Eqs. (26) so that all behavior constraints are written

$$\sum_{i=1}^{B}\sum_{j=1}^{4} C_{ijp}(X_{ij} - X_{0ij}) + C_{0q} \geq 0; \quad q = 1,\ldots,Q \tag{36}$$

Move Limits

Move limits on the RSP's are included to insure that any redesign move does not exceed the range of validity of the approximate problem. These are developed from user supplied constants C_y and C_x and the side constraints on the CSD's, Eqs. (11) and (12). The intermediate quantities $\tilde{Y}_{ik}^{(U)}$ and $\tilde{Y}_{ik}^{(L)}$ are defined

$$\tilde{Y}_{ik}^{(U)} = \min\{Y_{ik}^{(U)}, Y_{0ik}C_y\} \tag{37}$$

$$\tilde{Y}_{ik}^{(L)} = \max\{Y_{ik}^{(L)}, Y_{0ik}/C_y\} \tag{38}$$

These intermediate values are used with Eq. (24) to define move limits on X_{ij}

$$X_{ij}^{(U)} = \min\{f_{ij}(\tilde{Y}^{(L)}), f_{ij}(Y_0)C_x\} \tag{39}$$

$$X_{ij}^{(L)} = \max\{f_{ij}(\tilde{Y}^{(U)}), f_{ij}(Y_0)/C_x\} \tag{40}$$

Equations (39) and (40) are then used to form side constraints in RSP space.

$$X_{ij}^{(U)} - X_{ij} \geq 0 \tag{41}$$

$$X_{ij} - X_{ij}^{(L)} \geq 0 \tag{42}$$

Objective Function

Equations (20) and (21) are used to write the objective function, which is to be minimized.

$$\min_X \hat{M}(X) = \min_X \sum_{i=1}^{B} \frac{W_i}{X_{i1}} \tag{43}$$

where

$$W_i = \sum_{b \in T_i} \rho_b L_b \tag{44}$$

T_i represents the set of analysis elements that are linked to form the ith design element. Note that X_{i2}, X_{i3}, and X_{i4} do not appear in Eq. (43).

Because the DUAL2 optimizer requires an objective function which contains all the design variables, Eq. (43) is modified for use in the DUAL2 optimizer only

$$\min_X \hat{M}^{(D)}(X) = \min_X \sum_{i=1}^{B}\sum_{j=1}^{4} \frac{W_{ij}}{X_{ij}} \tag{45}$$

where W_{i2}, W_{i3}, and W_{i4} are small artificial masses. The existence of these artificial masses causes an alternation of the objective function contours, and may deflect the solution from the optimum, but experience has shown that the mass penalty is small, while the gain in efficiency, achieved by using the DUAL2 optimizer, is large.

Approximate Problem Restatement

NEWSUMT

Find X_{ij} such that

$$\min_X \sum_{i=1}^{B} \frac{W_i}{X_{i1}} \tag{46}$$

subject to behavior constraints

$$\sum_{i=1}^{B}\sum_{j=1}^{4} C_{ijq}(X_{ij} - X_{0ij}) + C_{0q} \geq 0; \qquad q = 1,\ldots,Q \tag{47}$$

Y side constraints

$$\sum_{i=1}^{B}\sum_{j=1}^{4} B_{ijp}\left(\frac{1}{X_{ij}} - \frac{1}{X_{0ij}}\right) + B_{0p} \geq 0; \qquad p = 1,\ldots,P \tag{48}$$

X move limits

$$X_{ij}^{(U)} - X_{ij} \geq 0; \qquad i = 1,\ldots,B \quad j = 1,2,3,4 \tag{49}$$

$$X_{ij} - X_{ij}^{(L)} \geq 0; \qquad i = 1,\ldots,B \quad j = 1,2,3,4 \tag{50}$$

DUAL2

Find X_{ij} such that

$$\min_X \sum_{i=1}^{B}\sum_{j=1}^{4} \frac{W_{ij}}{X_{ij}} \tag{51}$$

subject to behavior constraints

$$\sum_{i=1}^{B}\sum_{j=1}^{4} C_{ijq}(X_{ij}-X_{0ij})+C_{0q}\geq 0;\quad q=1,\ldots,Q \tag{52}$$

Y side constraints

$$\sum_{i=1}^{B}\sum_{j=1}^{4} \bar{B}_{ijp}(X_{ij}-X_{0ij})+\bar{B}_{0p}\geq 0 \tag{53}$$

X move limits

$$X_{ij}^{(U)}-X_{ij}\geq 0;\qquad i=1,\ldots,B\quad j=1,2,3,4 \tag{54}$$

$$X_{ij}-X_{ij}^{(L)}\geq 0;\qquad i=1,\ldots,B\quad j=1,2,3,4 \tag{55}$$

V. Optimizers

Two optimizers are provided for the solution of the approximate problem formed earlier. The NEWSUMT and DUAL2 codes have been reported previously, so their description here is brief.[1,2,13]

NEWSUMT

NEWSUMT is an extended quadratic interior penalty function optimizer. For an objective function $\hat{M}(X)$ [Eq. (46)] and constraints $f_l(X)$ representing Eqs. (47-50), the unconstrained penalty function is

$$P(X,r)=\hat{M}(X)+r\sum_{l=1}^{L}\bar{f}_l(X) \tag{56}$$

where $\bar{f}_l(X)$ is defined

$$\bar{f}_l(X)=\frac{1}{f_l(X)} \qquad ;\quad f_l(X)\geq\epsilon$$

$$=\frac{1}{\epsilon}\left[\left(\frac{f_l(X)}{\epsilon}\right)^2-\frac{3f_l(X)}{\epsilon}+3\right] \quad ;\quad f_l(X)<\epsilon \tag{57}$$

The parameters r and ϵ are calculated internally in NEWSUMT.

NEWSUMT has the capability of solving problems with nonlinear constraints, and, thus, is able to accommodate the nonlinear constraint set of Eqs. (48). NEWSUMT also has the attractive feature of providing a solution which is in the interior of the feasible region, so that intermediate solutions of the problem are likely to be feasible.

DUAL 2

The DUAL2 optimizer is highly efficient for two reasons; first, the optimizer deals with a constraint set which includes only the strictly active constraints, and, second, the recovery of the RSP's, internal to the optimizer, is a simple, closed-form calculation due to the algebraic structure of the approximate problem.

Defining F as the feasible region defined by Eqs. (54) and (55), and Q_r as the set of strictly active constraints, the dual variables, λ and γ, are to be found such that the dual function $l(\lambda,\gamma)$ is maximized

$$l(\lambda,\gamma)=\min_{X\in F}\left\{\sum_{i=1}^{B}\sum_{j=1}^{4}\left[\frac{W_{ij}}{X_{ij}}-\left(\sum_{q\in Q_r}\lambda_q C_{ijq}+\sum_{p\in Q_r}\gamma_p\bar{B}_{ijp}\right)\right.\right.$$

$$\left.\left.\times(X_{ij}-X_{0ij})\right]-\sum_{q\in Q_r}\lambda_q C_{0q}-\sum_{p\in Q_r}\gamma_p\bar{B}_{p0}\right\} \tag{58}$$

where Eqs. (52) and (53) define the coefficients. The minimization subproblem expressed in Eq. (58) is solved in closed form to define the RSP's as a function of λ and γ

$$(\tilde{X}_{ij})^2=-\left[\left(\sum_{q\in Q_r}\lambda_q C_{ijq}+\sum_{p\in Q_r}\lambda_p\bar{B}_{ijp}\right)\Big/W_{ij}\right] \tag{59}$$

$$X_{ij}=X_{ij}^{(L)};\ (\tilde{X}_{ij})^2\leq(X_{ij}^{(L)})^2$$

$$=\tilde{X}_{ij}\ ;\ (X_{ij}^{(L)})^2<(\tilde{X}_{ij})^2<(X_{ij}^{(U)})^2$$

$$=X_{ij}^{(U)};\ (X_{ij}^{(U)})^2\leq(\tilde{X}_{ij})^2 \tag{60}$$

Inspection of Eq. (59) demonstrates the requirement for artificial masses in the objective function for the DUAL2 optimizer. When the maximum of Eq. (58) has been found, the optimal RSP's are known for the approximate primal problem.

VI. Cross-Sectional Dimension Variable Recovery

The solution to the approximate problem is calculated in terms of the RSP's, while the variables of interest to the designer are the CSD's. Equations (29) or (33) are used to recover the CSD's. It is important to note that, since these are the same equations used to approximate the Y side constraints, the Y side constraints are satisfied if constraint Eqs. (30) or (34) are satisfied. Because the CSD side constraints have a strong effect on the solution of the problem, this exact representation has a beneficial influence on the convergence of the problem, while at the same time, it is unnecessary to resort to multilevel techniques to recover the CSD's.

VII. Flow Chart

The flow chart in Fig. 3 shows the combination of the various elements of the program package. Note that convergence is indicated by a sufficiently small relative mass change in two successive iterations. In the optimizer block, the selection of NEWSUMT or DUAL2 is determined by input data.

VIII. Numerical Examples

To show the usefulness of this approach, four sample design problems are solved, involving two different struc-

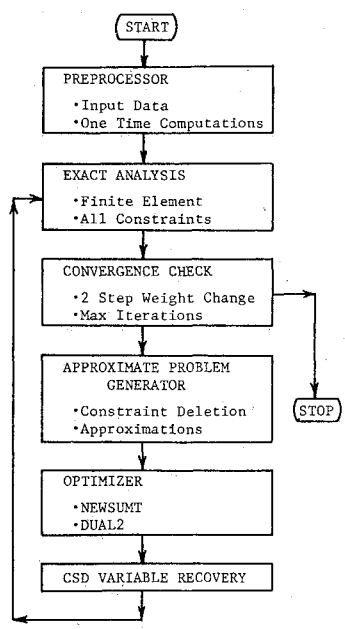

Fig. 3 Program block diagram.

tures. Each of the four problems is solved with both optimizers (NEWSUMT and DUAL2). All problems were solved using the IBM 3033 computer at UCLA.

It should be noted that the Fortran code was written with the intent that DUAL2 be the main optimizer. Therefore, only a minimal effort was made to present NEWSUMT with a well-scaled approximate problem, and the reported solution times may not accurately represent the full potential of NEWSUMT.

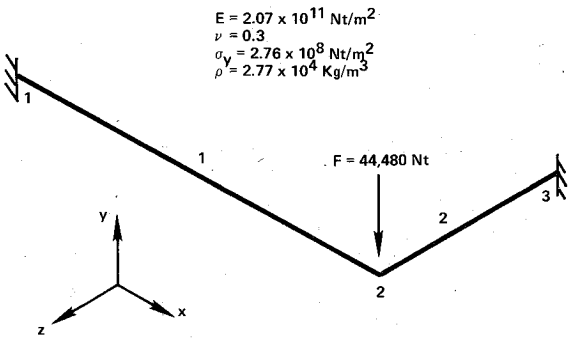

Fig. 4 Bartel structure.

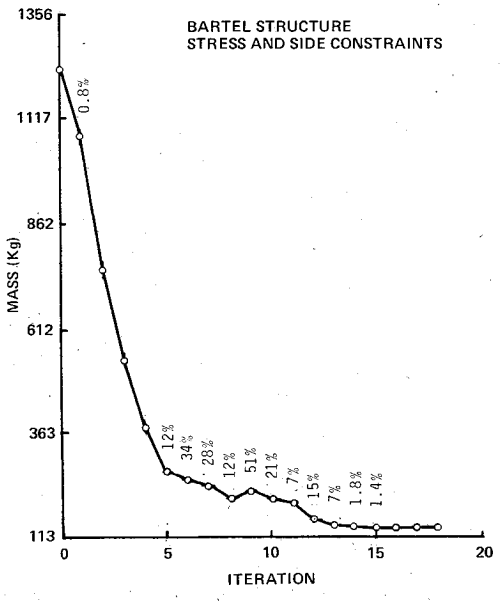

Fig. 5 Problem 1 iteration history DUAL2 optimizer.

Bartel Structure

The first structure is taken from Bartel.[7] This structure consists of two cantilevered beams lying in the x-z plane. The longer element is 2.54-m long, while the shorter element is 1.27-m long. Figure 4 shows this structure.

In Bartel's formulation, all wall thicknesses of each cross section are equal, so that the design is specified by three variables per member.

Problem 1

The first problem considers material stress and side constraints only, as posed by Bartel. Bartel's solutions found the optimal mass in the 131.1-132.4-kg range. Table 1 shows the initial and final designs as found by Bartel, as well as NEWSUMT and DUAL2 results obtained using the current method. Figure 5 shows the iteration history for the DUAL2 optimizer.

The percentages above the plotted points indicate the amount of violation of the most negative constraint at that iteration, as indicated by the exact constraint evaluation. Points that have no accompanying percentage are less than 0.1% infeasible, and they are considered to be feasible for practical purposes. This labeling practice is adopted for all mass iteration histories.

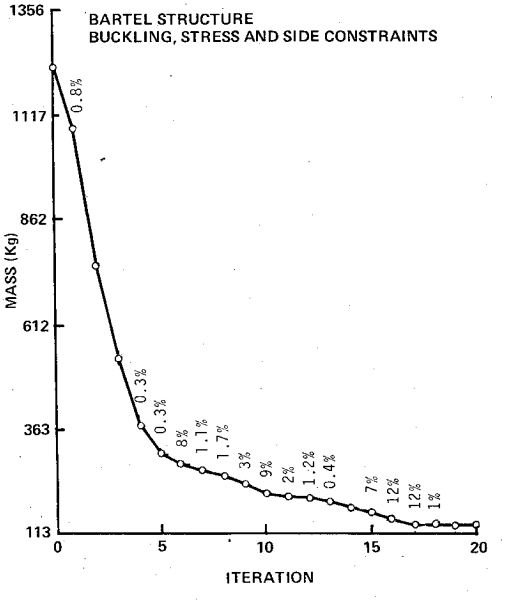

Fig. 6 Problem 2 iteration history DUAL2 optimizer.

Table 1 Problem 1 design variables (Y; B_i, H_i, t_{hi}, t_{bi})

	Bartel's solution, cm				NEWSUMT/DUAL2 solution, cm				
	Initial design	Lower bound	Final design	Upper bound	Initial design	Lower bound	NEWSUMT Final design	DUAL2 Final design	Upper bound
B_1	22.9	6.35	6.35	25.4	10.2	6.35	6.63	6.35	25.4
H_1	22.9	6.35	6.35	25.4	15.2	6.35	6.58	6.35	25.4
t_{h1}	2.29	0.254	0.254	2.54	2.03	0.254	0.254	0.254	2.54
t_{b1}	2.29	0.254	0.254	2.54	2.29	0.229	0.231	0.229	2.54
B_2	22.9	6.35	24.2	25.4	20.3	6.35	16.7	6.35	25.4
H_2	22.9	6.35	25.4	25.4	22.9	6.35	25.3	25.4	25.4
t_{h2}	2.29	0.254	0.254	2.54	2.03	0.254	0.254	0.254	2.54
t_{b2}	2.29	0.254	0.254	2.54	2.29	0.229	0.389	1.14	2.54
Final mass:	131.21 kg				Final mass:		NEWSUMT:	133.03 kg	
							DUAL2:	133.70 kg	
					Execution time:		NEWSUMT:	17.91 s	
							DUAL2:	1.47 s	

All three solutions show that the longer member should be at minimum gage design, while the shorter member's height (H_2) approaches its upper bound (25.4 cm). All solutions also agree that the stress at node 3 is the critical behavior constraint. The variations in the final design indicate that the optimum is rather "shallow" and the minimum mass material distribution may not be unique.

Note that the mass penalty in the DUAL2 solution, introduced by the artificial masses, is acceptably small, while the execution time for the DUAL2 optimizer is significantly shorter than that obtained with the NEWSUMT optimizer.

Problem 2

Analysis of Bartel's six design variable solution shows that the buckling constraints, as posed here, are seriously violated. In order to examine the mass penalty for inclusion of the buckling constraint, problem 1 is solved again, this time with buckling constraints considered. Figure 6 shows the mass history, and Table 2 shows the designs. These results indicate that the previously obtained optimum mass for the eight design variable problem, see Table 1, is unaffected by the buckling constraint. Although the NEWSUMT design is slightly altered, the DUAL2 design is unchanged. In fact, although the buckling constraint is not critical in the final design, it is critical in several intermediate designs, thus affecting the design history. Stress is again critical at node 3 in the final design.

2×5 Grillage

Moses and Onoda have presented results for various stress limited grillages.[6] A 2×5 grillage is selected from their work as a test problem. Figure 7 shows that structure which is in the x-z plane and subjected to a 175 N/cm distributed load on all members. Symmetry in both loading and design allows symmetric modeling of the structure. Because Moses and Onoda used a significantly different cross-sectional design, no comparison of solutions is presented here.

Problem 3

This problem considers nodal displacement and CSD side constraints only. Figure 8 shows the iteration history for the DUAL 2 optimizer, and Table 3 displays the design solution determined by each optimizer. Although the distribution of material differs in these two solutions, both solutions agree that the displacement constraints are active at nodes 7 and 10, and both final masses agree closely. Previous experience with displacement critical designs indicates that multiple designs all having essentially the same minimum mass can be expected.

Problem 4

The structure of problem 3 is solved again, but with local buckling, material stress, nodal displacement, and CSD side constraints included. The iteration history for the DUAL2 optimizer is shown in Fig. 9, and the solutions are shown in

Table 2 Problem 2 design variables (Y; B_i, H_i, t_{hi}, t_{bi})

	NEWSUMT solution, cm				DUAL2 solution, cm			
	Initial design	Lower bound	Final design	Upper bound	Initial design	Lower bound	Final design	Upper bound
B_1	10.2	6.35	6.60	25.4	10.2	6.35	6.35	25.4
H_1	15.2	6.35	6.65	25.4	15.2	6.35	6.35	25.4
t_{h1}	2.03	0.254	0.254	2.54	2.03	0.254	0.254	2.54
t_{b1}	2.29	0.229	0.230	2.54	2.29	0.229	0.229	2.54
B_2	20.3	6.35	14.1	25.4	20.3	6.35	6.35	25.4
H_2	22.9	6.35	25.3	25.4	22.9	6.35	25.4	25.4
t_{h2}	2.03	0.254	0.254	2.54	2.03	0.254	0.254	2.54
t_{b2}	2.29	0.229	0.467	2.54	2.29	0.229	1.14	2.54
Final mass:	133.45 kg				Final mass:	133.70 kg		
Execution time:	16.97 s				Execution time:	1.71 s		

Table 3 Problem 3 design variables (Y; B_i, H_i, t_{hi}, t_{bi})

	NEWSUMT solution, cm				DUAL2 solution, cm			
	Initial design	Lower bound	Final design	Upper bound	Initial design	Lower bound	Final design	Upper bound
B_1	43.2	2.54	45.7	48.3	30.5	2.54	16.0	48.3
H_1	48.3	2.54	50.8	50.8	38.1	2.54	48.0	50.8
t_{h1}	2.03	0.127	0.127	2.41	20.3	0.127	0.127	2.41
t_{b1}	2.41	0.114	0.144	2.54	2.41	0.114	0.114	2.54
B_2	43.2	2.54	47.8	48.3	30.5	2.54	16.8	48.3
H_2	48.3	2.54	50.8	50.8	38.1	2.54	39.9	50.8
t_{h2}	2.03	0.127	0.127	2.41	20.3	0.127	0.127	2.41
t_{b2}	2.41	0.114	0.132	2.54	2.41	0.114	0.114	2.54
B_3	43.2	2.54	45.7	48.3	30.5	2.54	34.3	48.3
H_3	48.3	2.54	50.8	50.8	38.1	2.54	50.8	50.8
t_{h3}	2.03	0.127	0.127	2.41	20.3	0.127	0.127	2.41
t_{b3}	2.41	0.114	0.876	2.54	2.41	0.114	2.09	2.54
B_4	43.2	2.54	48.3	48.3	30.5	2.54	12.4	48.3
H_4	48.3	2.54	50.8	50.8	38.1	2.54	50.8	50.8
t_{h4}	2.03	0.127	0.127	2.41	20.3	0.127	0.127	2.41
t_{b4}	2.41	0.114	1.44	2.54	2.41	0.114	2.52	2.54
Final mass:	3157 kg				Final mass:	3162 kg		
Execution time:	32.71 s				Execution time:	17.45 s		

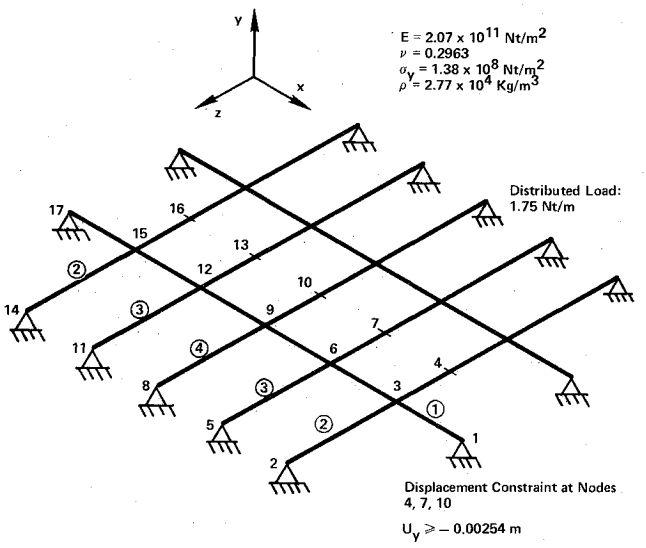

Fig. 7 2×5 grillage.

Table 4. The displacement constraints at nodes 7 and 10 are again critical, while no stress constraints are critical. Both solutions agree that buckling constraints are critical in the long member at nodes 3 and 15 and in the short members at nodes 6, 9, and 12, while only the NEWSUMT solution produces a critical buckling constraint at node 4. The masses of the two solutions again agree closely, even with this slight difference in the critical constraint set.

IX. Conclusions

A new approximation concepts design procedure that facilitates efficient minimum mass design of space frame structures has been presented. Optimization is carried out by treating a sequence of approximate problems posed in terms of reciprocals of the section properties. The design procedure generates cross-sectional dimensions without recourse to multilevel procedures. The key link between the section properties and cross-sectional dimensions is maintained by a periodically updated linearization. This method considers side constraints on the cross-sectional design variables and

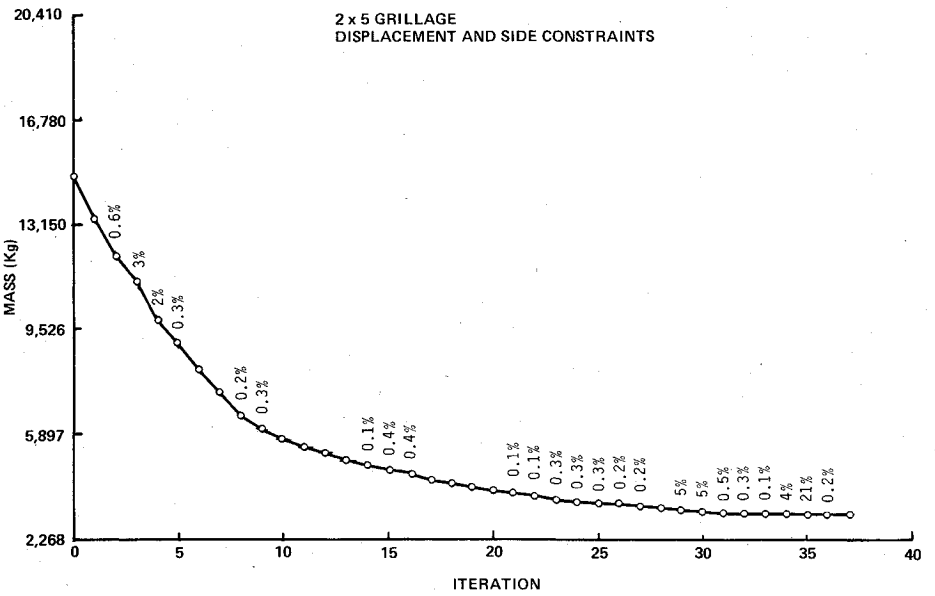

Fig. 8 Problem 3 iteration history DUAL2 optimizer.

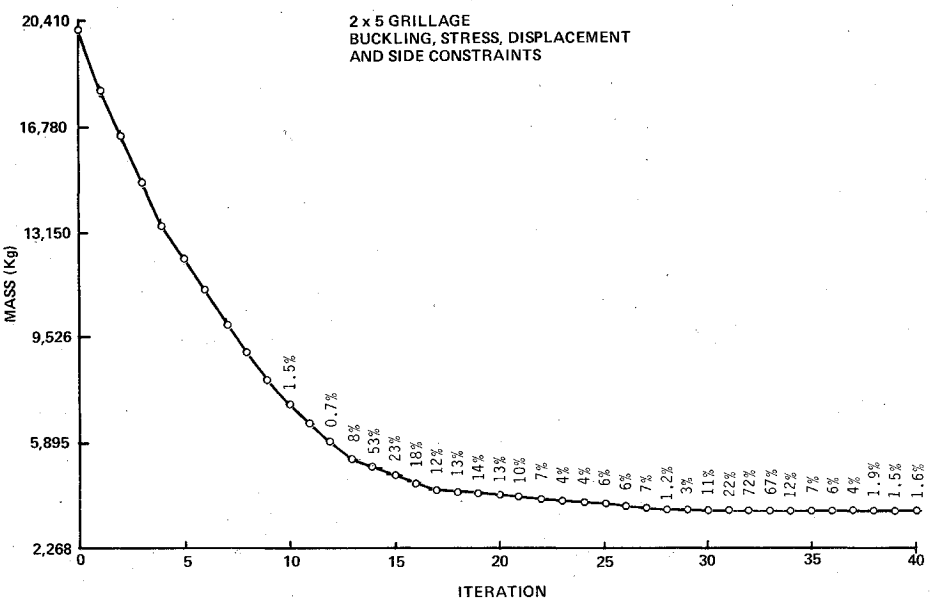

Fig. 9 Problem 4 iteration history DUAL2 optimizer.

Table 4 Problem 4 design variables (Y; B_i, H_i, t_{hi}, t_{bi})

	NEWSUMT solution, cm				DUAL2 solution, cm			
	Initial design	Lower bound	Final design	Upper bound	Initial design	Lower bound	Final design	Upper bound
B_1	43.2	2.54	33.5	48.3	43.2	2.54	15.5	48.3
H_1	48.3	2.54	50.5	50.8	48.3	2.54	50.8	50.8
t_{h1}	2.03	0.127	0.228	2.41	2.03	0.127	0.235	2.41
t_{b1}	2.41	0.114	0.292	2.54	2.41	0.127	0.404	2.54
B_2	43.2	2.54	29.5	48.3	43.2	2.54	21.0	48.3
H_2	48.3	2.54	50.5	50.8	48.3	2.54	38.6	50.8
t_{h2}	2.03	0.127	0.186	2.41	2.03	0.127	0.163	2.41
t_{b2}	2.41	0.114	0.239	2.54	2.41	0.127	0.188	2.54
B_3	43.2	2.54	47.2	48.3	43.2	2.54	16.1	48.3
H_3	48.3	2.54	50.8	50.8	48.3	2.54	50.8	50.8
t_{h3}	2.03	0.127	0.219	2.41	2.03	0.127	0.249	2.41
t_{b3}	2.41	0.114	0.488	2.54	2.41	0.127	2.54	2.54
B_4	43.2	2.54	48.0	48.3	43.2	2.54	29.2	48.3
H_4	48.3	2.54	50.8	50.8	48.3	2.54	50.8	50.8
t_{h4}	2.03	0.127	0.320	2.41	2.03	0.127	0.297	2.41
t_{b4}	2.41	0.114	1.86	2.54	2.41	0.127	2.54	2.54
Final mass:	3600 kg				Final mass:	3596 kg		
Execution time:	83.82 s				Execution time:	16.32 s		

behavior constraints, including material stress, local buckling, and nodal displacement and rotation constraints.

Solutions for four example problems have been presented, each with two different optimizers. In each case, the optimal masses found by the two optimizers agree well, and also agree with one comparable problem from the literature. All problems solved involve highly redundant structures, providing a good test of the usefulness of the method. Satisfactory convergence was observed in every case. Finally, the solutions are intuitively satisfying, generating designs that are conceptually similar to the solutions that a designer might select.

Appendix

Material Stress Constraints

For the frame element shown in Fig. 1, the material stress is checked at sixteen points. Figure A1 shows the node at one end of an analysis element and the forces and moments that are present, in local coordinates. For any frame element subject to the loads in Fig. A1, the maximum stress may occur at either end of the element being considered. Since each frame analysis element has four walls and two ends, the stress level is sampled at 16 locations in each analysis element. Figure A2 shows the eight points sampled for the end shown in Fig. A1. The normal stresses are obtained from elementary beam theory and the shear stresses are determined assuming the box beam section is thin walled. The normal and shear stresses in the ith element at the sample points shown in Fig. A2 are

$$\sigma_{p1} = \sigma_{p2} = \tfrac{1}{2}M_{1z}Y_{i2}X_{i3} + \tfrac{1}{2}M_{1y}Y_{i1}X_{i4} - F_{1x}X_{i1} \quad \text{(A1)}$$

$$\sigma_{p3} = \sigma_{p4} = -\tfrac{1}{2}M_{1z}Y_{i2}X_{i3} + \tfrac{1}{2}M_{1y}Y_{i1}X_{i4} - F_{1x}X_{i1} \quad \text{(A2)}$$

$$\sigma_{p5} = \sigma_{p6} = -\tfrac{1}{2}M_{1z}Y_{i2}X_{i3} - \tfrac{1}{2}M_{1y}Y_{i1}X_{i4} - F_{1x}X_{i1} \quad \text{(A3)}$$

$$\sigma_{p7} = \sigma_{p8} = \tfrac{1}{2}M_{1z}Y_{i2}X_{i3} - \tfrac{1}{2}M_{1y}Y_{i1}X_{i4} - F_{1x}X_{i1} \quad \text{(A4)}$$

$$\tau_{p8} = \tau_{p1} = -\frac{M_{1x}}{2Y_{i1}Y_{i2}Y_{i4}} - \frac{F_{1z}}{2Y_{i1}Y_{i4}} \quad \text{(A5)}$$

$$\tau_{p2} = \tau_{p3} = -\frac{M_{1x}}{2Y_{i1}Y_{i2}Y_{i3}} - \frac{F_{1y}}{2Y_{i2}Y_{i3}} \quad \text{(A6)}$$

$$\tau_{p4} = \tau_{p5} = \frac{M_{1x}}{2Y_{i1}Y_{i2}Y_{i4}} - \frac{F_{1z}}{2Y_{i1}Y_{i4}} \quad \text{(A7)}$$

$$\tau_{p6} = \tau_{p7} = \frac{M_{1x}}{2Y_{i1}Y_{i2}Y_{i3}} - \frac{F_{1y}}{2Y_{i2}Y_{i3}} \quad \text{(A8)}$$

Since the box beam walls are subject to combined stress [normal (σ) plus shear (τ)] the following specialized form of the distortion energy yield criterion is employed:

$$\sigma^2 + 3\tau^2 \le \sigma_y^2 \quad \text{(A9)}$$

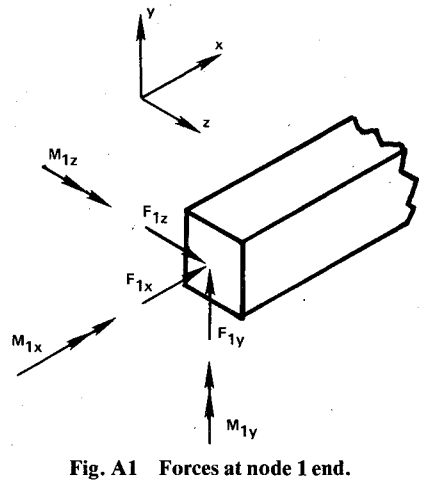

Fig. A1 Forces at node 1 end.

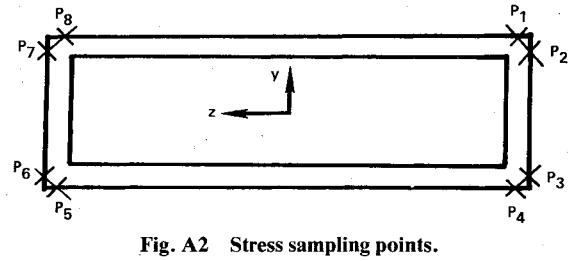

Fig. A2 Stress sampling points.

where σ_y is the yield stress for the material. This is placed in the standard constraint form and normalized

$$1-\frac{1}{\sigma_y^2}(\sigma^2+3\tau^2)\geq 0 \tag{A10}$$

To find the value of the stress constraint at location P1, Eqs. (A1) and (A5) are substituted into Eq. (A10)

$$1-\frac{1}{\sigma_y^2}\left[(\tfrac{1}{2}M_{1z}Y_{i2}X_{i3}+\tfrac{1}{2}M_{1y}Y_{i1}X_{i4}-F_{1x}X_{i1})^2 +3\left(-\frac{M_{1x}}{2Y_{i1}Y_{i2}Y_{i4}}-\frac{F_{1z}}{2Y_{i1}Y_{i4}}\right)^2\right]\geq 0$$

In a similar manner, a total of 16 stress constraint equations are formed to monitor the stress state at all potentially critical locations.

Local Buckling Constraint

To protect against buckling any of the four box beam walls subjected to the stresses as described in the previous section, each side of the frame member is modeled as an infinitely long, simply supported plate. The simply supported assumption is conservative. The assumption of an infinitely long plate neglects stiffening effects due to the end boundary conditions—an assumption which is also conservative.

Figure 2 shows the three types of plane stress distribution that can exist in any plate under the assumptions made herein. For buckling critical stresses τ_{cr}, σ_{xcr}, and σ_{bcr}, define the buckling stress ratios

$$R_S=\tau/\tau_{cr} \tag{A11}$$

$$R_b=\sigma_b/\sigma_{bcr} \tag{A12}$$

$$R_x=\sigma_x/\sigma_{xcr} \tag{A13}$$

The critical stresses are given by Gerard and Becker.[9] For an infinitely long plate of width b and thickness t

$$S=\frac{E}{12(1-\nu^2)}\left(\frac{\pi t}{b}\right)^2 \tag{A14}$$

$$\tau_{cr}=5.35S \tag{A15}$$

$$\sigma_{bcr}=23.9S \tag{A16}$$

$$\sigma_{xcr}=4S \tag{A17}$$

The three buckling ratios are then combined in one interaction formula to form the local buckling constraint

$$1-R_x-R_b^2-R_s^2\geq 0 \tag{A18}$$

To compute the value of the buckling constraint for the side between points P8 and P1 in Fig. (A2) at the node end in Fig. (A1), Eqs. (A1-A13) are used.

$$1-\left[\frac{\dfrac{-M_{1z}Y_{i2}X_{i3}}{2}+F_{1x}X_{i1}}{4S}\right]-\left[\frac{-\tfrac{1}{2}M_{1y}Y_{i1}X_{i4}}{23.9S}\right]^2 -\left[\frac{\dfrac{M_{1x}}{2Y_{i1}Y_{i2}Y_{i4}}+\dfrac{F_{1z}}{2Y_{i1}Y_{i4}}}{5.35S}\right]^2\geq 0 \tag{A19}$$

Acknowledgment

This research was supported by NASA Research Grant NSG 1490.

References

[1] Miura, H. and Schmit, L. A., "NEWSUMT—A Fortran Program for Inequality Constrained Function Minimization—User's Guide," NASA CR 159070, June 1979.

[2] Fleury, C., "Structural Weight Optimization by Dual Methods of Convex Programming," *International Journal for Numerical Methods in Engineering*, Vol. 14, Dec. 1979, pp. 1761-1783.

[3] Isreb, M., "Three Dimensional Beam Elements Synthesis Applications with Stress Constraints, Nonlinear Size-Stiffness Relationships and Various Size-Inertia Powers," *Computers & Structures*, Vol. 7, Aug. 1977, pp. 565-569.

[4] Isreb, M., "DESAPI: A Structural Synthesis with Stress and Local Instability Constraints," *Computers & Structures*, Vol. 8, April 1978, pp. 243-256.

[5] Fleury, C., "Large Scale Structural Optimization by Finite Elements," *Proceedings, International Symposium on Optimum Structural Design, The 11th ONR Naval Structural Mechanics Symposium*, U. S. Office of Naval Research and University of Arizona College of Engineering, Oct. 1981, pp. 11.23-11.41.

[6] Moses, F. and Onoda, S., "Minimum Weight Design of Structures with Application to Elastic Grillages," *International Journal for Numerical Methods in Engineering*, Vol. 1, Oct.-Dec. 1969, pp. 311-331.

[7] Bartel, D. L., "Optimum Design of Spatial Structures," Ph.D. Dissertation, University of Iowa, 1969.

[8] Bennett, J. A., "Application of Linear Constraint Approximation to Frame Structures," *Proceedings, International Symposium on Optimum Structural Design, The 11th ONR Naval Structural Mechanics Symposium*, U. S. Office of Naval Research and University of Arizona College of Engineering, Oct. 1981, pp. 7.9-7.15.

[9] Gerard, G. and Becker, H., "Handbook of Structural Stability, Part I—Buckling of Flat Plates," NACA TN 3781, July 1957.

[10] Fleury, C. and Schmit, L., "ACCESS 3—Approximation Concepts Code for Efficient Structural Synthesis—User's Guide," NASA CR 159260, Sept. 1980.

[11] Schmit, L. A. and Farshi, B., "Some Approximation Concepts for Structural Synthesis," *AIAA Journal*, Vol. 12, May 1974, pp. 692-699.

[12] Fuchs, M. B., "Linearized Homogeneous Constraints in Structural Design," *International Journal of Mechanical Sciences*, Vol. 22, Jan. 1980, pp. 33-40.

[13] Fleury, C. and Schmit, L. A., "Dual Methods and Approximation Concepts in Structural Synthesis," NASA CR 3226, Dec. 1980.